

# A novel technique for synthesis of silver nanoparticles by laser-liquid interaction

R. SUBRAMANIAN, P. E. DENNEY, J. SINGH

*Applied Research Laboratory, The Pennsylvania State University, University Park, PA 16804, USA*

*E-mail: JXS46@psu.edu*

M. OTOONI

*US Army Armament Research, Development and Engineering Center, Picatinny Arsenal, NJ 07876, USA*

---

Ultrafine particles of many materials have received much attention over the last few years by researchers because of their unique physical and mechanical properties due to increased surface area to volume ratio. A novel laser-liquid interaction technique has been developed to synthesize silver nanoparticles from inexpensive silver nitrate solution in distilled water. The shape, size distribution, microchemistry and crystal structure of the silver nanoparticles were studied using X-ray diffraction, scanning electron microscopy and electron probe X-ray microanalysis. © 1998 Kluwer Academic Publishers

---

## 1. Introduction

Sub-micrometre ( $< 100 \text{ nm} < \text{diameter} < 1 \mu\text{m}$ ) and nanoscale ( $1 \text{ nm} < \text{diameter} < 100 \text{ nm}$ ) particles are receiving much attention in both basic science and advanced technological research. There has been a growth in the production of clusters and nanocrystalline materials for potential catalytic, sensor, aerosol, filter, biomedical, magnetic, dielectric, optoelectronic, structural, ceramic and metallurgical applications. In this nanoscale regime, particles exhibit volume and surface effects that are absent in the same material with dimensions in the micrometre range [1–5]. Nanoscale particles have unique physical properties (e.g. optical, dielectric, magnetic, mechanical), transport properties (e.g. thermal, atomic diffusion), and improved processing characteristics (e.g. faster sintering kinetics, super-plastic forming). For some applications, a narrow size distribution is required to obtain a uniform materials response.

Materials such as paints, pigments, electronic inks, and ferrofluid, as well as advanced functional and structural ceramics, require that the particles be uniform in size and stable against agglomeration. Fine particles, particularly nanoscale particles with significant surface area, often agglomerate to minimize the total surface or interfacial energy of the system. Although solution chemistry can be a practical route for the synthesis of both sub-micrometre and nanoscale particles of many materials, issues such as the control of size distribution of particles, morphology and crystallinity, particles agglomeration during and after synthesis and separation of these particles from the reactants, need further investigation.

The usual synthesis techniques for producing nanoparticles include mechanical milling of solid

phases, solution chemistry and vapour-phase synthesis. Nanostructured particles have also been synthesized by chemical techniques such as chemical precipitation [6], and sol-gel processing [7]. Vapour deposition of particles has been achieved by gas evaporation [9], laser ablation [10] and sputtering [11]. The advantages and disadvantages of these processes are summarized in Table I. The method of production of nano-particles in each of these processes is described below.

### 1.1. High-energy milling process

In this method, micrometre-sized crystallites are repeatedly deformed and eventually disintegrate completely into nanosized grains. The production of a wide variety of nanostructured materials using mechanical energy has been termed mechano-synthesis. It is essentially a dry, high-energy ball-milling process performed close to room temperature, without supplying any external heat. This process does not generally involve chemical change. The mechano-synthesis of nanophase materials is effected by the direct synthesis of compounds from elemental powders or by various exchange, transfer, and mixing reactions initially involving compounds. Among the many different types of nanophase materials synthesized by this process are stable, meta-stable, mixed and novel carbides with crystal sizes between 10 and 20 nm. For example nanostructured carbide of titanium, zirconium, hafnium, vanadium, niobium, etc.; silicides of iron, cobalt, nickel, chromium, etc.; aluminides of iron, titanium, nickel, etc. have been made by this process [12–20].

TABLE I Advantages and disadvantages of the methods for making nanocrystalline particles

Method	Advantages	Disadvantages
Mechanical milling	High production rates	Contamination, limited multi-components
Thermal	Simple system	Non-reactive, limited multi-component, materials produced, moderate production rates
Electron beam	Limited reaction	Low production rates, limited multi-component materials produced, vacuum unit required
Laser ablation	Reactive, quenching complex, multi-component materials, produced	Low production rates, vacuum unit required
Gas phase precursor	High production rates, reactive, multi-component materials produced	Complex system (control of reaction and particle size in series difficult), precursor choice, no quenching, vacuum unit required
Flame pyrolysis	High production rates, reactive, multi-component materials produced	Complex system (control of reaction and particle size in series difficult), precursor choice, no quenching, vacuum unit required
Laser pyrolysis	High production rates, reactive, multi-component materials produced	Low production rates, complex system (control of reaction and particle size in series difficult), precursor choice, no quenching, vacuum unit required
Colloidal	High production rates, reactive, multi-component materials produced	Solvent extraction (contamination)

## 1.2. Solution chemistry

Solution chemistry provides a cost-effective method for the production of large quantity of nanoparticles. A unique feature offered by solution chemistry is the ability to manipulate matter at the molecular level. As a result, better chemical homogeneity of materials can be achieved. When the relationship between the molecular level of assembly of matter and its macroscopic properties is understood, synthetic chemistry can be tailored to prepare target materials. There is an increasing interest in multi-disciplinary approaches in metal synthesis and processing, integrating solution chemistry and bimolecular science [6,7].

The stabilization of fine particles requires the formation of repulsive inter-particle forces. The choice of surfactant always depends on the type of materials to be synthesized or dispersed. To synthesize stabilized, uniformly fine particles, colloidal chemistry offers a possible route. For instance, ferrofluids of amorphous iron nanoscale particles [21] and ceramic hydroxides [22] have been prepared. Colloidal stability can be achieved by either synthesizing the particles in the presence of surfactant, or by dispersing as-synthesized particles in surfactant [21–23]. A surfactant is a surface-active agent that has an amphipatic structure in a solvent under its conditions of use (i.e. a lyophobic solvent attractive).

## 1.3. Chemical vapour phase condensation methods

In these methods, atoms, which are formed by evaporation, agglomerate and condense into clusters in a low-pressure inert-gas atmosphere. The clusters are transported by convection to a liquid nitrogen-cooled cold finger, where they are collected for further processing.

Spray pyrolysis is also a processing route to form nanoparticles. Spray pyrolysis is an aerosol process wherein a metal salt solution is atomized into droplets

and sent through a hot-wall reactor. Inside the reactor the solvent evaporates and the metal salt decomposes to form the product particles. The powder characteristics and production rate depends upon many factors including droplet size, residence time, precursor solution concentration, reaction atmosphere and temperature. This technique has been utilized to produce solid spherical, nanosized metals (e.g. silver, molybdenum etc.), oxides ( $V_2O_5$ , PdO,  $YBa_2Cu_3O_{7-x}$  etc.), nitride ( $Si_3N_4$ ), carbonitrides [Si(C,N)], ceramic/metal composites (WC-Co,  $Al_2O_3$ , Fe/Cr) [20–30]. For example, nanosized silver metal particles were produced from  $AgNO_3$  (silver nitrate) solution with an ultrasonic generator at and above  $600^\circ C$  using nitrogen carrier gas, and at and above  $900^\circ C$  using air as the carrier gas. A common problem cited in the spray pyrolysis is the formation of porous particles after solvent evaporation and reaction, and this was reduced by using an aqueous-ethanol precursor solution [31]. Formation of nanoparticles of  $Ag_2O$  and  $AgNO_3$  was also reported. As the precursor solution concentration was increased from 0.5 M to 0.4 M, the particle size also increased from  $1.03 \mu m$  to  $1.68 \mu m$  for the ultrasonic generator.

Nanocrystalline metals made by the vapour phase condensation method are very reactive and have also been used for ceramic compounds which were reported to be formed by introducing reactive gases into the synthesis chamber. The reactants (precursor chemicals) can be in several forms: vapour, aerosol, gel, crystalline powder, amorphous powder, liquid solution, colloidal solution, and so forth. The reactants are heated by an energy source, such as laser, flame, furnace, etc. The laser is found to be a more versatile tool for the synthesis of materials as compared to other heat-energy sources.

The capability of lasers as a tool for materials processing has already been demonstrated [32–42]. Laser chemical vapour deposition (LCVD) and laser physical vapour deposition (LPVD) techniques can produce thin (tens of nanometres to hundreds of

micrometres) layers of metals, semiconductors and ceramics with precise spatial control [36–38]. Metals and ceramics can be co-deposited using this technique to produce composites. Use of lasers as the energy source has been found to be more efficient (up to 10,000 times faster deposition rate) than conventional Chemical Vapor Deposition (CVD) technique. The LCVD process can be classified into three categories: (i) pyrolysis, (ii) evaporation and (iii) photolysis, depending upon the reaction mechanism. Details of these processes are summarized below.

### 1.3.1. Pyrolytic LCVD

In the production of nano-crystalline materials by pyrolytic LCVD, the laser beam impinges upon the substrate, and results in heating of the area exposed. The heating is a result of a number of processes such as energy transfer from high-energy electrons, non-radioactive recombination and vibrational lattice excitation. Thermal decomposition of the reactant gases takes place in the vicinity of this localized region. The laser wavelength is chosen so that it is absorbed by the substrate and not by the reactant gases.

When a pulse laser heats a surface the material remains at a high temperature for a very short duration (for e.g., 7 nsec pulses at  $\lambda = 1.06 \mu\text{m}$  leaves a Si surface molten for  $\sim 40$  nsec [39]). Since the gas-surface impingement is negligible in this short time period, deposition over large areas cannot be carried out using pulse laser. Also, in the case of pulse laser, high repetition rates (MHz) are required since the fractional duty cycle is quite small. Therefore a laser operating in continuous wave mode is necessary. The requirements of CW laser are the light absorption at the wave length used and the laser power must be adequate to heat the illumination area to a temperature sufficient to induce thermal decomposition. In pyrolytic LCVD, thermal decomposition is usually the dominant mechanism. In addition, the photons present in a wide range of energies can also induce gas-phase dissociation of reactants via multiple photon processes. The laser requirements for pyrolytic decomposition are easily met with a number of commercially available lasers (e.g.,  $\text{CO}_2$  or Ar-ion lasers).

### 1.3.2. Evaporative LPVD Process

In the evaporative LPVD process, a laser beam is directed onto a solid target and the high flux of photons removes atoms from the target as in conventional evaporation or ion-sputter deposition. The atoms are subsequently transported towards the substrate kept close to the target. It has been established that the ejected atoms leave the surface with a distribution more forward-peak energy (i.e., thermal) than the typical cosine-squared distribution found in conventional evaporation [34, 35]. The forward peaked distribution may detrimentally affect film uniformity and step coverage.

Since, lasers are available in a broad spectrum of wavelengths, pulse energies and pulse widths, it is envisioned that with the choice of appropriate laser,

the LPVD technique can be used to deposit thin films of almost any material. The versatility of this technique is reflected by the fact that almost 128 different materials have been deposited in thin film form by LPVD technique [36]. The unique features of this process are lower deposition temperature, lower impurity contents, and equiaxed grain structure. LPVD offers many advantages over conventional physical vapor deposition techniques. The LPVD technique can produce energetic (10 to 100 eV) ionized and excited vapor species which can enhance the surface mobility and re-crystallization process and thus lower the growth temperature. Undesirable impurities, such as oxygen, can be minimized during the decomposition process by maintaining an inert atmosphere or high vacuum inside the processing chamber. In addition, the substrate will be at a low temperature ( $< 400^\circ\text{C}$ ) and the heating of the target occurs in a spatially selective region inside the vacuum chamber. This process is fully compatible with the high-vacuum system since the laser beam is generated outside the vacuum system. LPVD provides instantaneous control of the ablation process and the film thickness from near atomic to micro dimensions by choosing appropriate laser parameters.

### 1.3.3. Laser photolytic CVD process (gas media)

Production of nanocrystalline materials by this process occurs when a laser beam is absorbed by gaseous species in a single or multi-photon process. The absorption leaves the donor molecule in an excited state which, if above the dissociation limit, can cause the molecule to fragment. Products of this photo-dissociation, then, either react chemically with other species present or condense on a nearby surface. This type of LCVD can be used to deposit both fine lines or uniform thin films over large areas ( $> 10 \text{ cm}^2$ ). The laser processing parameters are beam energy, wavelength, and mode of laser operation (pulse or continuous wave), and whether or not the laser light impinges on the substrate.

Chemical vapour deposition can be enhanced by the addition of photons to photo-dissociate reactant molecules [37]. Laser photons have a wide energy distribution in the range 0.1–7.0 eV and above 7 eV in the ultraviolet. Because these photon energies are in excess of the bonding energies of many molecules, reactant molecules undergo decomposition by absorbing photons. Selective output products by the dissociation of the reactant molecules can be achieved due to the narrow energy spectrum of the photons in contrast to dissociation by electron impact. In addition, the output of a laser can be manipulated both temporally and spatially, providing additional flexibility to the photo-deposition process. Owing to these unique advantages of using lasers, the laser CVD provides a new method for the synthesis of materials.

Because photolytic LCVD relies on the photo-dissociation of gas-phase donor molecules, a different set of laser properties is required. The most critical

parameter is the wavelength of the light used. The laser can be operated in pulsed or continuous wave mode. The reactant molecules are raised to unstable excited states, due to absorption of photons. The molecules release excess energy by splitting into fragments. This process is termed photofragmentation. A photon density sufficient to pump large numbers of molecules into the excited states is required to achieve high deposition rates over a large area. This subsequently results in dissociation of molecules at high energy and nanoscale particle formation.

The laser photolytic process is a non-equilibrium thermodynamic process. Interaction of a reactant gas stream with the pulsed high-power infrared CO<sub>2</sub> laser creates a rapid heating/cooling rate ( $10^5$  °C s<sup>-1</sup>) in the reaction zone for the production of nanoscale particles. A variety of nanoscale particles has been produced using this technique and includes Si, SiC, SiN [39–41], ZrB<sub>2</sub> [43], TiO<sub>2</sub> [44, 45],  $\alpha$ -Fe [46], Cr, Mo, W [47], etc. Ultrafine (< 10 nm) elemental powders were produced by laser-induced breakdown of metal carbonyl vapours [48]. Size and synthesis reaction rate depend upon the reaction parameters used to synthesize nanoparticles such as laser intensity, wavelength, beam diameter, nozzle diameter, chamber pressure, and gas flow rate (C<sub>2</sub>H<sub>4</sub>, CH<sub>4</sub>, etc.).

In the pyrolytic LCVD process, the substrate is heated with a laser beam and a chemical reaction takes place at the gas–solid interface near the hot spot where the film is deposited. Chemical reaction or decomposition takes place in the gaseous environment. Therefore, the synthesis rate of nanoparticles is very low and a vacuum unit is required. Besides gas, a liquid medium can also be used for the synthesis of materials. Very little or no research has been directed to the laser-assisted synthesis of nanoscale materials using liquid media.

## 2. Experimental procedure

A schematic diagram of the experimental setup used in the production of nanoscale particles by laser beam–liquid interaction is shown in Fig. 1. The solution used consisted of AgNO<sub>3</sub> (silver nitrate) dissolved in distilled water which was taken in the reaction chamber. A rotating stainless steel substrate was immersed in the silver nitrate solution and was irradiated by the laser beam. The laser processing parameters used in the present investigation are given below:

type and mode of laser: CW CO<sub>2</sub> laser;

laser beam power: 275, 300, 400 W;

laser-beam focus condition, at focused and defocused conditions (beam diverged through the substrate);

laser beam diameter: 3 mm;

interaction time: 3 and 7 min.

Continuous rotation of the substrate during laser–liquid interaction distributes the powder particles formed in the solution and prevents agglomeration due to further interaction with the laser beam. Synthesized nanoparticles were separated by a centrifugal separator at 2000 r.p.m. Synthesized nanoparticles were characterized by various techniques.

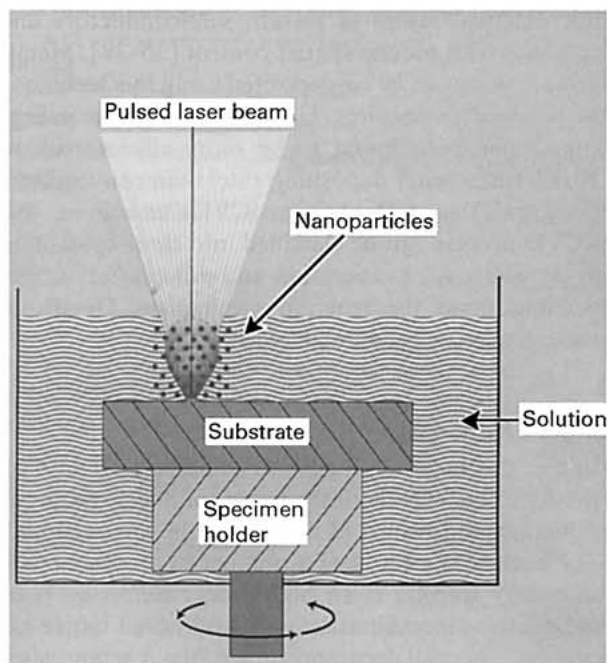


Figure 1 Schematic representation of the novel laser–liquid–solid interaction technique.

X-ray diffraction analysis of the nano-particles was carried out using CuK radiation with a single crystal monochromator. Characteristic Bragg diffraction angles in the X-ray diffraction profile obtained from the silver powder sample were compared with the silver-standard diffraction profile.

The size, shape and distribution of the nanoparticles produced were examined using the JOEL JSM-6300F high-resolution scanning electron microscope (SEM) equipped with the field emission gun. The microchemistry of the nanoparticles was determined using a Cameca SX-50 electron microprobe equipped with energy dispersive spectrometer. The wavelengths and energies of the X-ray characteristics of the elements in the powder sample were measured and the elements present were identified.

## 3. Results and discussion

Fig. 2 shows a scanning electron micrograph of the nano-crystalline silver particles synthesized from silver nitrate solution using a focussed CW CO<sub>2</sub> laser-beam at a power of 275 W and an exposure time of 3 min. The average size of nanoparticles was about 20 nm. The corresponding X-ray diffraction pattern obtained from the powder is displayed in Fig. 3 indicating that silver nanoparticles are crystalline in nature. Fig. 3 also shows an X-ray diffraction pattern taken from the anhydrous silver nitrate crystals (starting material). The same silver-powder samples were further examined in the electron microprobe. The X-ray microchemical data obtained from the nanoparticles using the electron microprobe are shown in Fig. 4. The characteristic peaks from the elemental silver have been identified. The absence of characteristics peaks from nitrogen and oxygen indicates that the powder particles produced are free from oxygen (i.e. oxide

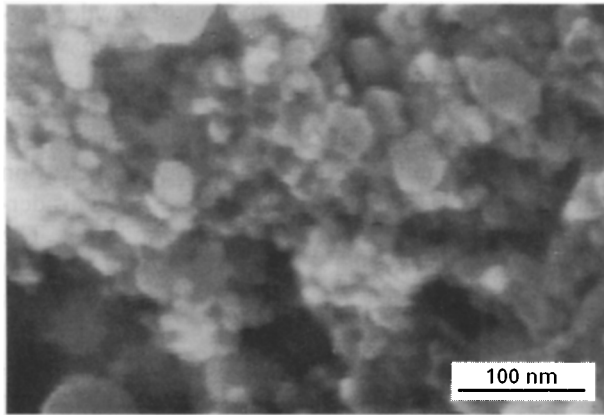


Figure 2 Scanning electron micrograph showing nanocrystalline silver particles synthesized from silver nitrate solution by the laser-liquid interaction.

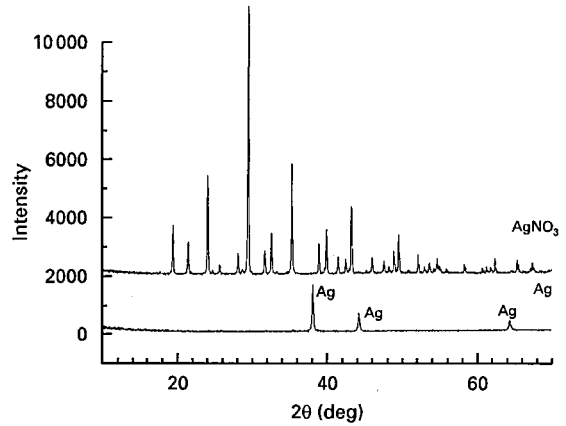


Figure 3 X-ray diffraction analysis showing pure silver particles recovered from silver nitrate solution.

formation) and nitrogen. Thus, high-quality silver nano particles were formed by this novel laser-liquid interaction technique.

Fig. 5 shows a scanning electron micrograph of the nanocrystalline silver particles produced from the silver nitrate solution using a focussed CW CO<sub>2</sub> laser-beam at a power of 300 W and an exposure time of 3 min. Relatively large nanospherical particles were synthesized in the size range from 100–1000 nm. In addition, agglomerated nanoparticles have also been found under these conditions.

Fig. 6 shows a scanning electron micrograph of the silver particles produced at a beam-powder of 300 W

and a longer exposure time of 7 min. The major portion of the nanoparticles produced is an agglomerated mass along with some spherical particles of size 100–1000 nm. This can be explained by the fact that a higher exposure time resulted in the interaction of the laser beam with the nanoparticles, which caused agglomeration.

Fig. 7 shows a scanning electron micrograph of the nanocrystalline silver particles formed by this technique using the CO<sub>2</sub> laser beam at a power of 400 W, a defocused beam diameter of 3 mm and an exposure time of 3 min. Recirculation of the solution has been used to produce these powder particles.

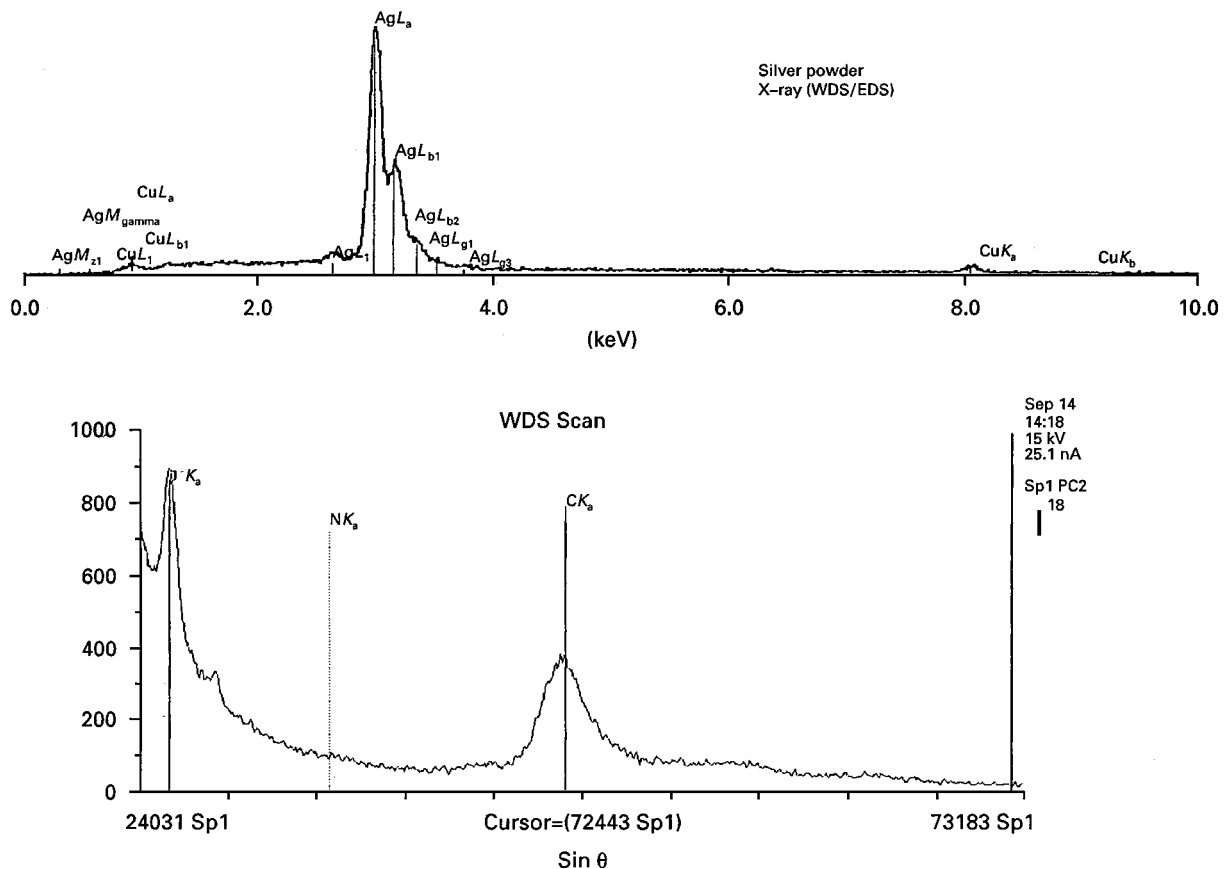


Figure 4 Energy dispersive X-ray microchemical data obtained from the silver particles in the electron microprobe.

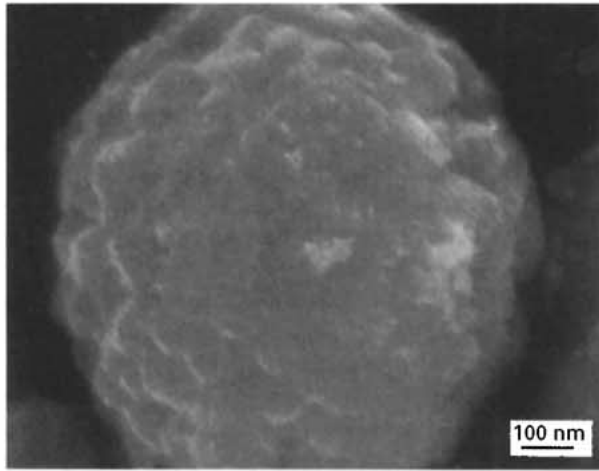


Figure 5 Scanning electron micrographs showing nanocrystalline silver particles formed from silver nitrate solution by laser-liquid interaction (focused CW CO<sub>2</sub> laser beam with power 300 W, exposure time 3 min).

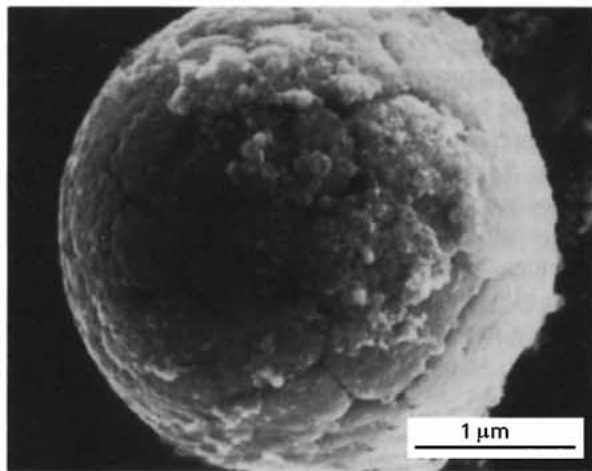


Figure 6 Scanning electron micrograph showing nanocrystalline silver particles formed from silver nitrate solution by laser-liquid interaction (focused CW CO<sub>2</sub> laser beam with power 300 W, exposure time 7 min)

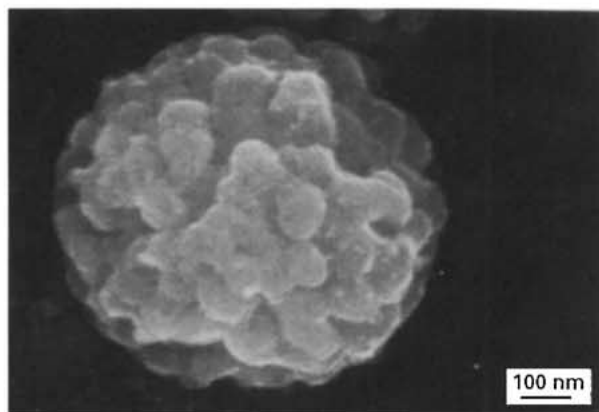


Figure 7 Scanning electron micrograph showing nanocrystalline silver particles formed from silver nitrate solution by laser-liquid interaction (defocused CW CO<sub>2</sub> laser beam with power 400 W, exposure time 3 min).

It can be seen from the microstructure that, due to re-exposure of the reaction solution to the laser beam, subsequent nucleation and growth of new spherical particles on the particles already formed has taken

place. This results in the production of powder particle clusters in the size range 100–1000 nm which consist of several layers of spherical particles. The formation of such particles can be explained as follows. A spherical particle that was formed already by the nucleation and growth, acts as a site for nucleation for several new spherical particles which are considerably smaller in size and of the order of 10 nm. The shape of these special type particles differs from that of the agglomerated particles produced by this technique.

By this novel laser-liquid interaction technique, high-quality nanocrystalline particles were synthesized in the size range 20–100 nm at a rate of 3–6 g min<sup>-1</sup>. The size, shape, synthesis rate and microstructure of silver nanoparticles were found to be dependent upon the laser processing conditions and interaction time. A similar finding was reported by Singh and Vellaikal [49] in the synthesis of nanocrystalline diamond from liquid benzene.

The nucleation and growth mechanism in the formation of micrometre and submicrometre sized metal particles by the solution chemistry technique, has been reported [50]. In this laser-liquid interaction technique, the silver metal atoms are generated in the liquid phase, and once the supersaturation is high enough, nucleation and growth of silver nanoparticles occur. The nanoparticles produced by the laser-liquid interaction technique are highly spherical and are homogeneous in size. The final size of the metal particles obtained is formed from the nuclei which have been nucleated at the same time and have grown simultaneously. These particles are then homogeneous in size. Under these conditions, the nucleation is homogeneous and the nuclei appear spontaneously.

#### 4. Conclusions

Successful production of nano-scale silver particles from the silver nitrate solution by the laser beam-liquid interaction method has been reported in this paper. The size of nanoparticles varied from 10–1000 nm, depending upon the laser processing conditions, including laser beam power, beam diameter, laser interaction time and the concentration of the reaction solution. X-ray diffraction and electron microprobe results from the nanoparticles indicated that high-quality silver particles were produced.

The laser beam-liquid interaction technique for the production of ultrafine particles has several unique advantages over other methods described in this paper. Highly spherical particles of many metals in the nanoscale regime can be produced by the careful optimization of these process parameters.

#### References

1. C. HAYASHI, *Phys. Today* December (1997) 44.
2. *Idem.*, *J. Vac. Sci. Technol.* A5 (1987) 1375.
3. N. ICHINOSE, Y. OZAKI and S. KASHU, "Superfine particles Technology" (Springer London, 1992).
4. H. GLEITER, *Nano-struct. Mater.* 1 (1992) 1.
5. A. H. HEUER *et al.*, *Science* 255 (1992) 1098.
6. Z. X. TANG *et al.*, *J. Coll. Interface Sci.* 146 (1991) 38.

7. D. W. HOFFMAN *et al.*, *J. Am. Ceram. Soc.* **67** (1984) 468.
8. E. HELLSTERN *et al.*, *J. Appl. Phys.* **65** (1989) 305.
9. Y. KAWAMURA *et al.*, *Mater. Sci. Eng.* **98** (1988) 449.
10. M. L. MANDICH *et al.*, *J. Chem. Phys.* **86** (1987) 4245.
11. F. H. KAATZ *et al.*, *J. Mater. Res.* **8** (1993) 995.
12. S. W. LYONS, L. M. WANG and T. T. KODAS, *Nano-struct. Mater.* **2** (1992) 37.
13. A. H. CARIM, P. DOHERTY, T. T. KODAS and K. OTT, *Mater. Lett.* **8** (1989) 335.
14. W. SYMONS, S. C. DANFORTH, in "Proceedings of the Third International Conference Ceramic on Materials and Components for Engines", edited by V. J. Tennery (American Ceramics Society, Westerville, OH, 1989) p. 67.
15. K. E. GONSALVES, P. R. STRUTT, T. D. XIAO and P. G. KLEMENS, *J. Mater. Sci.* **27** (1992) 3231.
16. D. SEYFERTH and G. H. WISEMAN, *J. Am. Ceram. Soc.* **67** (1984) C132.
17. T. D. XIAO, K. E. GONSALVES, P. R. STRUTT and P. G. KLEMENS, *J. Mater. Sci.* **28** (1992) 1334.
18. K. YAHIKOZAWA, K. YASUDA and Y. MATSUDA, *Electrochem. Acta* **37** (1992) 453.
19. D. C. DOUGLASS *et al.*, *Phys. Rev. Lett.* **68** (1992) 1774.
20. M. G. BAWENDI *et al.*, *ibid.* **65** (1990) 1623.
21. H. GLEITTER, *Prog. Mater. Sci.* **33** (1989) 223.
22. M. ALPER, *MRS Bull.* November (1992) 53.
23. J. H. FENDLER, *Chem. Rev.* **87** (1987) 877.
24. S. MANN *et al.*, *MRS Bull.* October (1992) p. 32.
25. P. C. EKLUND *et al.*, *J. Mater. Res.* **8** (1993) 1666.
26. G. M. CHOW *et al.*, *J. Metals* November (1993) 2.
27. JUBIAN P. PARTRIDGE, *Mater. Res. Soc. Symp. Proc.* **129** (1989) 469.
28. S. KOMARNENI, *J. Mater. Chem.* **2** (1992) 1219.
29. S. KOMARNENI, *et al.*, *J. Mater. Res.* **8** (1993) 3176.
30. T. C. PLUM *et al.*, *J. Aerosol Sci.* **24** (1993) 383.
31. T. T. KODAS, in "Powder Processing", edited by F. Y. Wang (Elsevier, Amsterdam).
32. J. SINGH, *J. Metals* September (1992) 8.
33. J. SINGH *et al.*, NASA Technical Report 108431.
34. J. SINGH and J. MAZUMDER, *Acta Metall.* **35** (1987) 1995.
35. *Idem.*, *Metall. Trans.* **18** (1987) 313.
36. S. D. ALLEN, *J. Appl. Phys.* **52** (1981) 6501.
37. W. B. CHOU *et al.*, *J. Appl. Phys.* (1988).
38. J. SINGH *et al.*, *ibid.* **73** (1993) 4351.
39. R. SOLANKI *et al.*, *Solid State Technol.* July (1985) 220.
40. M. HANABUSA *et al.*, *Appl. Phys. Lett.* **38** (1984) 385.
41. G. P. DAVIS *et al.*, *J. Appl. Phys.* **56** (1984) 1808.
42. J. SINGH, in "Proceeding of NATO-ASI Conference on Materials and Processing for Surface and Interface Engineering", edited by Y. Pauleay, Series-E, Vol. 290 (Kluwer Academic, 1994) p. 347.
43. J. S. HAGGERTY, in "Laser-Induced Chemical Processes", edited by J. I. Steinfeld (Plenum Press, New York, 1981).
44. G. W. RICE and R. L. WOODIN, *J. Am. Ceram. Soc.* **71** (1988) C181.
45. F. CURCIO *et al.*, *Appl. Surface Sci.* **46** (1990) 225.
46. X. X. BI *et al.*, *J. Mater. Res.* **8** (1993) 1666.
47. S. M. SHIN *et al.*, *Mater. Lett.* **3** (1985) 265.
48. S. T. LIN and A. M. RONN, *Chem. Phys. Lett.* **56** (1978) 414.
49. J. SINGH and M. VELLAIKAL, in "Proceeding of the International Conference on Beam Processing of Advanced Materials", edited by J. Singh and S. Copely (TMS, 1993) p. 383.
50. F. FIEVET, J. P. LAGIER, B. BIN, B. BEAUDOIN and M. FIGLARZ, *Solid State Ionics* **32/33** (1989) 198.

*Received 19 April 1996  
and accepted 11 February 1997*